IEEE Access
Multidisciplinary | Rapid Review | Open Access Journal

Received June 13, 2019, accepted June 20, 2019, date of publication July 1, 2019, date of current version August 29, 2019.

Digital Object Identifier 10.1109/ACCESS.2019.2925771

Novel Method to Simultaneously Adjust the Size and pH Value of Individual Microdroplets in Silicone Oil

GENGCHAO CHEN[1], XIANMIN ZHANG[1], AND NING LI[2,3]

[1]Guangdong Key Laboratory of Precision Equipment and Manufacturing Technology, School of Mechanical and Automotive Engineering, South China University of Technology, Guangzhou 510640, China
[2]Department of Computer and Software Engineering, Institute of Biomedical Engineering, Polytechnique Montréal, Montréal, QC H3T 1J4, Canada
[3]Le Centre de recherche du CHUM (CRCHUM), Université de Montréal, Montréal, QC H2X 0A9, Canada

Corresponding author: Xianmin Zhang (zhangxm@scut.edu.cn)

This work was supported by the National Natural Science Foundation of China under Grant 51820105007.

ABSTRACT In this paper, a strategy to modify each micro-droplet's volume and synchronously adjust its pH value as required based on the electrolysis reaction in silicone oil is demonstrated. A pair of platinum electrodes fixed onto the jaws of a vernier caliper was used to modify the micro-droplet's volume and adjust its pH value by simply adjusting the distance between the two electrodes. To get a micro-droplet with desirable volume and pH values, three models, the relationship between the droplet's volume and its diameter when the droplet was placed on a fluorinated ethylene propylene (FEP)–covered glass substrate, the relationship between the distance of the two electrodes and the size of the resulted micro-droplet, and the relationship between the pH value and the micro-droplet's consuming rate, were built through the least square method. In our experiments, a droplet (5% sodium chloride solution, 1.4 uL, pH = 7) could consume 98.9% of its initial volume and form a new droplet with a volume of 0.016 μL and pH of 12.2. In addition, to validate that this method is also suitable in the acid and alkaline solutions, 0.001 mol/L NaOH and H_2SO_4 solutions were, respectively, operated using the same procedure. Both the volume and pH values could be controlled, which proved the potential application of our proposed method in analytical chemistry, precision engineering, and so on.

INDEX TERMS Microdroplet, electrolysis, pH value.

I. INTRODUCTION

Micro-sized water droplets have been widely used in multiple research fields, such as analytical chemistry [1], [2], precision engineering [3]–[7], biological sciences [8]–[12], etc. [13]–[17]. In these droplet-based applications, for smoothing the edge of a substrate processed by wet etching [18], digitally studying pH-sensitive enzymatic activities [19], [20] and precisely actuating intelligent structures made up of hydrogel and graphene [21]–[26], it is critical to produce ultra-mono-sized droplets with an exact pH value.

However, currently, it is still a big challenge to achieve the goal explained above. Generally, to form size-controllable and pH-desirable microdroplets, the current methods mainly rely on making the desired pH solution and then cutting it into smaller parts. To cut a droplet from a liquid phase, energy needs to be introduced to the cut-off point of the droplet surface so that some of the energy can be converted into the surface energy. Numerous principles have been proposed to generate the needed energy in order to precisely control the cut-off point [27]–[30]. The common energy that has been used to achieve the "break" function contains internal energy of liquids, such as hydrodynamic pressure [31]–[33], and external energy, such as electric energy [34], [35], magnetic energy [36], [37], thermal energy [38], [39], mechanical energy [40]–[43], etc. [44], [45]. According to different physical principles, each of these methods has its own advantages. In the control method relying on the internal energy of the liquid, such as hydrodynamics, the needed devices can have a simple structure, thereby making them low-cost [31]–[33]. However, due to the fact that liquids are subjected to friction forces when flowing through the inner wall of the tubes,

The associate editor coordinating the review of this manuscript and approving it for publication was Sanket Goel.

it is very difficult to control the break-off point of liquids precisely [31], [45]. In the electric control, the size of the produced micro-droplet is easily controlled by simply tuning the magnitude of power voltage [34], [35]. However, for this method, the manipulated solution is often limited to conductive liquids [45]. The magnetic control is only suitable to cut ferrofluids [36], [37], [45]. The thermal control method relies on micro-heater and temperature sensor to precisely change the viscosity and interfacial tension of liquids, which makes the fabrication complex and high-cost [38], [39], [45]. Although the laser has been tested to replace the micro-heater and temperature sensor in the thermal control method, the high-cost laser devices are difficult to be afforded for a common lab [45], [46]. The mechanical control method usually relies on pneumatically or hydraulically driving valves to cut the continuous liquid in the micro-fluidic devices. The principle makes this method suitable to most liquids [42], [43]. However, due to the fact that the gas is easy to be compressed in the valve and the liquid is suffered to friction forces when flowing through the inner wall of the valve, it is very difficult to control the break-off point precisely [45]. The acoustic pressure has also been tested to control the break-off point of liquids. In this method, the acoustic wave, excited by an interdigitated transducer (IDT), is used to cut the liquid contactlessly, which makes this method suitable in biology [40], [41]. However, the fabrication of IDT is very complicated, which hinders the wide use of this technology [45]. In summary, the cutting methods available lack the ability to form high-precision microdroplets in a common lab. Moreover, these methods are not capable of adjusting pH values and sizes after droplet formation.

In this paper, we propose and investigate a strategy to modify the size of droplets while simultaneously adjusting their pH value based on the electrolysis of water droplets in silicone oil. Considering the fact that, generally, making a bigger droplet can have a better control accuracy than forming a smaller microdroplet, our experimental hypothesis is that a size-controllable, pH-desirable microdroplet can be obtained through electrolysis of a big droplet. Here, there were still two monumental obstacles before this research: 1) How to acquire the volume of a droplet during electrolysis reactions, which is used to judge if the droplet has reached the desired volume; 2) How to know the initial droplet volume in order to make satisfying sizes and pH values in our demand. To solve these two questions, we built three mathematical models: 1) Based on the experimental results, a mathematical model (Model1) was built to calculate the current droplet volume using the droplet's diameter observed from an optical microscope; 2) Based on Model#1, we derived the relationship (Model#2) between the electrodes' distance and the resulted droplet volume. 3) Through the demanded droplet's sizes and pH values, the third model (Model#3) was used to calculate the required initial droplet volume. Thus, to form a microdroplet with a specific size and pH value, Model3 can be used to calculate the initial volume, and then, we need to set the appropriate electrodes' distance which is calculated by Model#2. When the desired droplet was obtained, electrolysis reactions stopped automatically, because the droplet was then too small to connect the two electrodes.

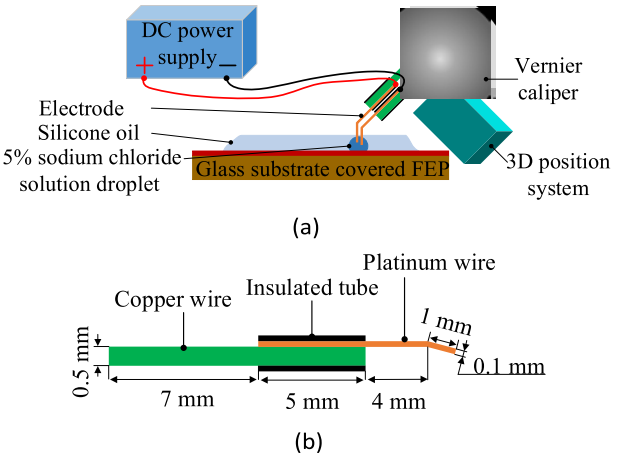

FIGURE 1. Experimental setup for modifying the droplet volume and pH values in silicone oil based on the electrolysis of the sodium chloride solution. (a) Experimental setup. (b) Size and composition of each electrode.

II. EXPERIMENT AND PHENOMENON

A. STRUCTURE

The experiment is conducted under an optical microscope (Microscopy system: Micromate 3X, Navitar, USA, Objective lens: Mitutoyo, Japan). The setup is shown in Fig. 1(a). In our experiments, a vernier caliper is fixed onto a 3D position system to adjust the spatial position easily. Then, two identical electrodes are fixed onto two ends of jaws which can precisely adjust the relative distance between the two electrodes. The structure and composition of each electrode are shown in Fig. 1(b). For each electrode, a platinum wire (length: $l = 10$ mm, electrical resistivity: $\rho = 105$ nΩ/m) is connected to a copper wire (diameter: $D = 0.5$ mm, $l = 12$ mm, $\rho = 17.2$ nΩ/m). The connected part of these two wires above, coated with insulated tubes, has a length of 5 mm. The two copper wires are respectively connected to the positive and negative terminals of a DC power supply (UPT3305, UNI-T, China). The tip of each platinum wire is bent perpendicularly with a bent length of 1 mm. Before being inserted into a droplet, the platinum wires are cleaned sequentially by a hydrochloric acid solution (5 mol/L), distilled water, acetone (Guangzhou reagent chemical factory, China) and isopropyl alcohol (Chengdu Jinshan Chemical Reagent Company Ltd., China) in an ultrasonic bath, and finally dried by nitrogen gas.

B. PHENOMENON AND THEORY

Fig. 2(a) is an illustration of the steps as explained above. Before our experiments, the electrodes were moved over a droplet and then moved down until they were inserted into the droplet with a set depth (about 400 μm). After switching on the power supply, numerous bubbles were generated on

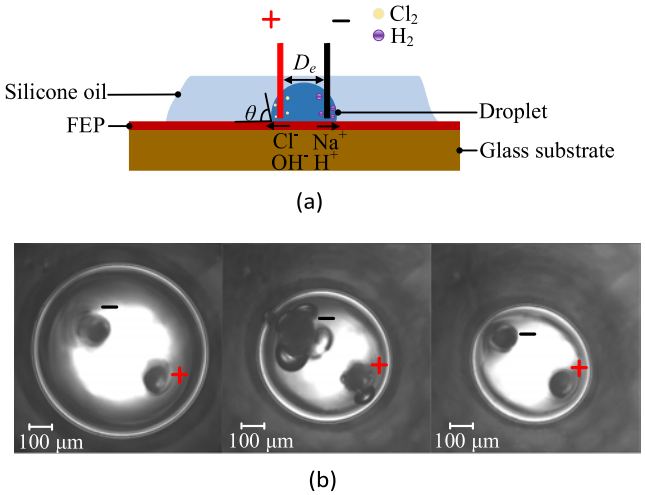

FIGURE 2. Illustration of the experiment. (a) Diagram of the setup. (b) Top-view images showing the steps involved in the modifications of the droplet's size in silicone oil before (left, 813 μm), during (middle, 631 μm) and after (right, 542 μm) the experiment.

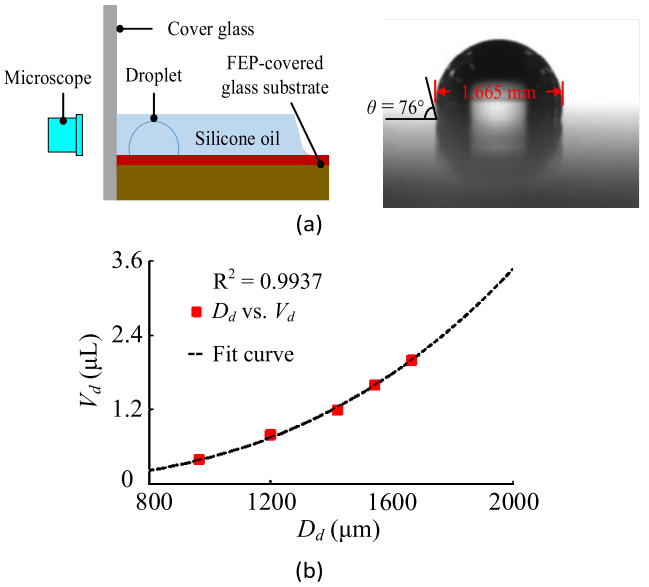

FIGURE 3. The side-view image of a 2 μL droplet and the relationship between the droplet's volume and its diameter after being placed on the FEP-covered glass substrate. (a) The setup for observing the droplet (left) and the obtained image (right). (b) Experimental results and a fitted curve showing the relationship between the droplet's volume and its diameter.

the anode and cathode due to the electrochemical reaction as (1) in the droplet. As the generated hydrogen (on the cathode) and chlorine bubbles (on the anode) constantly went up to the liquid surface, the droplet size slowly expanded when new bubbles were generated and rapidly shrank when the bubbles were released into the air, as shown in Fig. 2(b). The pH value of the droplet was expected to increase during the experiment, due to the generation of a sodium hydroxide solution, which can be seen in (1).

$$\begin{aligned}&\text{Anode}: 2Cl^- + 2OH^- \leftrightarrow 2e^- + Cl_2(g) + 2OH^-\\&\text{Cathode}: 2Na^+ + 2H^+ + 2e^- \leftrightarrow H_2(g) + 2Na^+\\&\text{Net}: 2NaCl(l) + 2H_2O(l) \leftrightarrow 2NaOH(l) + H_2(g) + Cl_2(g)\end{aligned} \tag{1}$$

After the droplet was modified to the required size, switched off the power supply and transferred the droplet to a neutral/stable place by moving the pair of electrodes. Fig. 2(b) shows a series of snapshots to demonstrate the different stages when modifying the droplet's size in silicone oil. During the experiments, the ambient temperature and pressure were 25 C° and 1 atm, respectively.

III. RESULT AND DISCUSSION

A. DROPLET'S DIAMETERS VS. ITS DIAMETER (D_d)

When a small droplet is in oil and on a substrate, it is difficult to measure the droplet's volume directly. Here, a mathematical model (Model # 1) was built to calculate the droplet's volume using its diameter observed microscopically (Microscopy system: Micromate 3X, Navitar, USA, Objective lens: Mitutoyo, Japan).

In the experiment, a droplet (5% sodium chloride solution) was generated through a microliter syringe (Shanghai Anting microliter syringe factory, China). The droplet was covered by a silicone oil (Tianjin Fuchen chemical reagents factory, China) film after being placed on a FEP-coved glass substrate. The contact angle meter (JC2001D, Shanghai Powereach Digital Technology Equipment Company Ltd.) was used to measure the droplet's contact angle (π - θ) with the substrate surface. Fig. 3(a) shows the side-view image of a 2 μL droplet after being placed on the glass substrate. To avoid the light distortion induced by the curved surface of the oil film, a cover glass was vertically adhered onto the FEP-covered glass subtract, as shown in Fig. 3(a). It can be clearly seen that the shape of the droplet looks like an asymmetric spherical cap.

Then, we set the droplet volume between 0.4 μL and 2.0 μL with increments of 0.4 μL. To build the relationship between the droplet's volume (V_d) and its diameter (D_d, top view, see Fig. 2), the least square method was used. The fitted curve is shown in Fig. 3(b) and the equation is as follows,

$$V_d = 0.138^*\pi^*D_d^3 \tag{2}$$

where V_d is the volume of the droplet and D_d is its diameter.

B. CONTROL OF THE DROPLET'S VOLUME BY TUNING THE DISTANCE BETWEEN THE TWO ELECTRODES

The possibility of controlling the droplet's volume was tested by tuning the distance between the two electrodes. With the progress of the electrolysis reaction, the droplet's size becomes smaller. When the size is smaller than that of the two electrodes, the droplet will be disconnected from the electrodes, resulting in the termination of the electrolysis reaction. Thus, by controlling the distance between the two electrodes, the droplets of desirable volume can be expected.

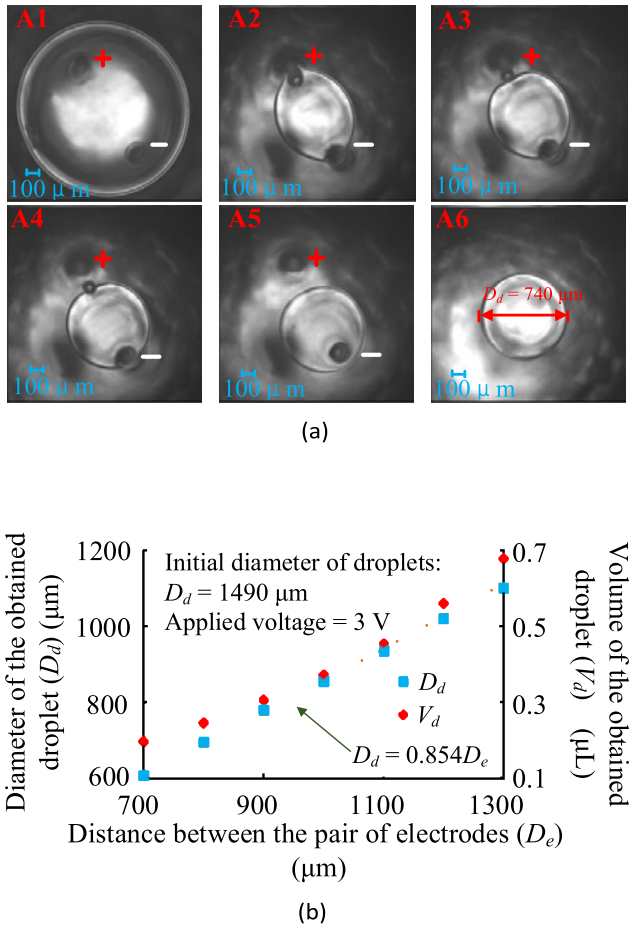

FIGURE 4. Controlling the volume of the resulted droplet by setting the distance of two electrodes. (a) Images showing the steps of modifying the droplet's size. (b) Electrodes' distance vs. droplets' diameter.

To validate our hypothesis above, two electrodes with a distance of 900 μm were inserted into a droplet (1.4 uL, 1490 μm) in a symmetrical manner (see image A1 in Fig. 4(a)). In Fig. 4(a), images A1-A6 show the droplet before and after being disconnected from one electrode. Here, an important phenomenon needs to be listed and explained here. Before a droplet is disconnected from the electrodes, the droplet does not have a circular shape but an oval shape (top-view). The "elongating effect" is probably induced by the intermolecular attraction between liquids and electrodes.

Fig. 4(a) A2-A5 shows the elongating droplet returned to the circle shape in 1.4 s. After removing the negative electrode from the droplet, the V_d can be calculated by measuring D_d and using (2). To compare the relationship between D_d and the D_e, in our experiments, seven droplets (1.4 uL, 1490 μm) were electrolyzed and the corresponding D_e was set to 700 μm-1300 μm with increments of 100 μm. The results are shown in Fig. 4(b). This figure shows that the obtained droplets always had a smaller size than D_e. However, these two parameters have a strong linear dependency (Model2), which validates our hypothesis that, by controlling the distance between electrodes, droplets with desirable volumes can be obtained.

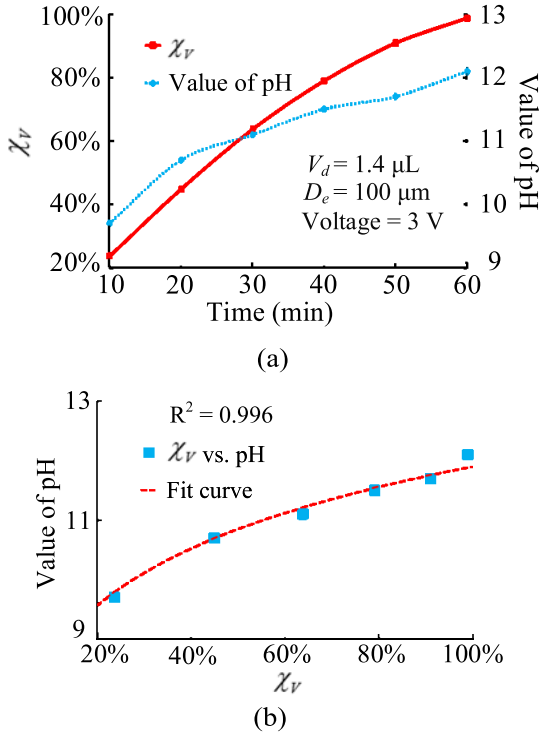

FIGURE 5. (a) The pH value and size of modified droplets (original diameter is 1.49 mm) vs. time. (b) The relationship between the resulted pH value and X_V.

C. SIMULTANEOUS CONTROL OF THE DROPLET SIZES AND pH VALUES

The pH values of 6 droplets (1.4 uL, 1490 μm) were tested using pH tested papers (Shanghai SSS Reagent Company Ltd, China) after being electrolyzed for 10-60 mins with increments of 10 mins. During the experiments, the distance between the two electrodes was set to100 μm. In the measurements, the lower end of the pH paper was inserted into the oil film, and then electrolyzed droplets were dragged by the electrodes until contact with the papers. The results are shown in Fig. 5(a). It can be clearly seen that the pH value increases when the consuming volume of the droplet increases. For the particle that was electrolyzed for 60 mins, the pH value reached 12.2 and the droplet size was 340 μm. The volume of this droplet was only 0.016 μL (1.1% of the initial volume) when calculated using (2). The experiment reveals that this method is capable of adjusting the pH values and sizes for a droplet at the same time.

In Fig. 5(b), by using the least square method, the relationship (Model3) between the resulted pH value and χ_v (the ratio of the consuming volume of a solution based on electrolysis to the initial volume) was built based on our experimental results shown in Fig. 5(a), which could be expressed as:

$$\mathrm{pH} = 11.82 + 3.744 * \lg(\chi_v + 0.05) \tag{3}$$

The χ_v is expressed as:

$$\chi_v = (V_i - V_s)/V_i \tag{4}$$

TABLE 1. The time required to modifying to a droplet to the specific sizes.

D_i	D_s	Time
1490 μm	1300 μm	58min
1490 μm	1200 μm	1h 23min
1490 μm	1100 μm	1h 45min
1490 μm	1000 μm	2h 4min
1490 μm	900 μm	2h 23min
1490 μm	800 μm	2h 41min
1490 μm	700 μm	2h 58min

where V_i and V_s are the initial and desired volume of micro-droplets, respectively.

According to (2), (3), (4) and model # 2, when V_i is fixed, the pH value of micro-droplet can be controllable just by setting the distance between two electrodes. To get a micro-droplet with the desirable pH value, the distance should be set:

$$D_e = [V_i^*[1.05 - 10^{(\mathrm{pH}-11.82)/3.744}]/(0.138 * \pi)]^{1/3}/0.854 \tag{5}$$

In addition, based on (3) and (4), to get a specific droplet with the desirable pH and volume, the needed V_i before the electrolysis reaction should be

$$V_i = V_s/[1.05 - 10^{(\mathrm{pH}-11.82)/3.744}] \tag{6}$$

D. VALIDATION OF THE MODODEL # 1, 2 AND 3 IN ALKALINE AND ACID SOLUTION (NaOH SOLUTION H_2SO_4 SOLUTION)

In the validation of these models, the experiment used the same setup, operational processes and experimental conditions, as what we did in section A, B and C above. The parameters of the used droplets are listed in table 1. However, in the model#3, different from the sodium chloride solution, these two solutions only consume water under electrolysis reactions, thus the NaOH solution results into an increased pH value while the H_2SO_4 solution concludes into a decreased pH liquid.

$$\mathrm{NaOH}: \mathrm{pH} = 14 + \lg[c_{NaOH}/(1 - \chi_v)] \tag{7}$$

$$\mathrm{H_2SO_4}: \mathrm{pH} = -\lg[(1 + \eta)^* c_{H_2SO_4}/(1 - \chi_v)] \tag{8}$$

where c_{NaOH} is the initial molar concentration of NaOH, $c_{H_2SO_4}$ is the initial molar concentration of H_2SO_4 and η is the ionization rate of HSO_4^- in DI water.

When V_i is fixed, for these two solutions, to get a micro-droplet with desirable pH value, the distance between the two electrodes should be set:

$$D_e = [V_i/10^{\mathrm{pH}-14} * c_{NaOH}/(0.13 * \pi)]^{1/3}/0.862 \tag{9}$$

$$D_e = [V_i/10^{-\mathrm{pH}} * (1+\eta)c_{H_2SO_4}/(0.13 * \pi)]^{1/3}/0.847 \tag{10}$$

In addition, to get a desirable droplet for these two solutions, the needed V_i should be:

$$V_i = V_s^* 10^{\mathrm{pH}-14}/c_{NaOH} \tag{11}$$

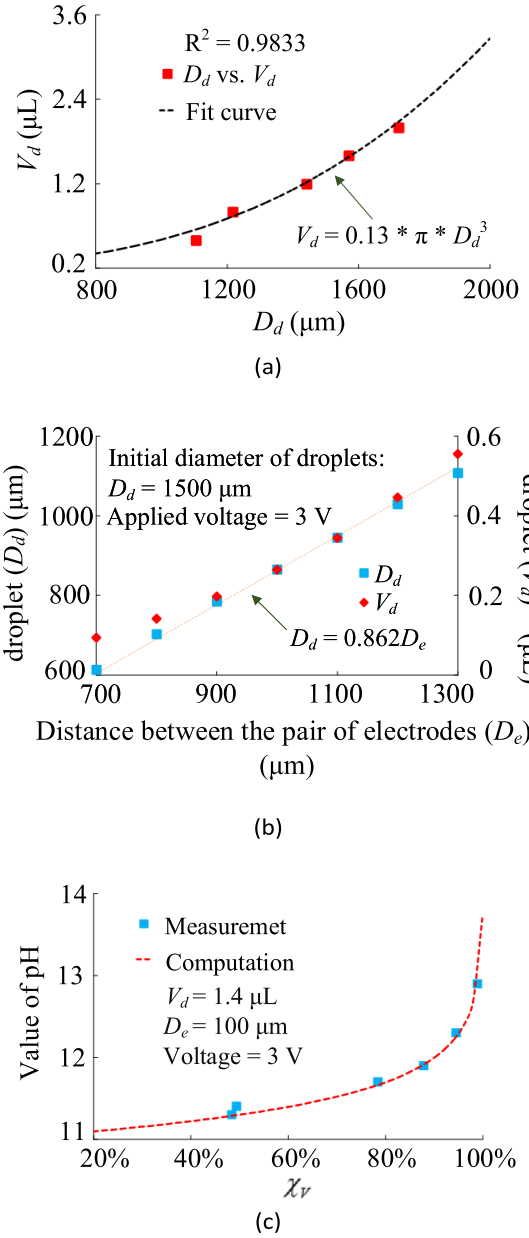

FIGURE 6. Demonstration of model #1, 2 and 3 in NaOH solution (0.001mol/L). (a) Relationship between the droplet's volume and its diameter. (b) Electrodes' distance vs. droplets' diameter. (c) The relationship between the resulted pH value and X_v.

$$V_i = V_s^* 10^{-\mathrm{pH}}/(1 + \eta)c_{H_2SO_4} \tag{12}$$

E. COMPARISON OF THREE MODELS IN THE THREE DIFFERENT SOLUTIONS ABOVE

In Fig. 8(a), the theoretical model# 1 obtained in Fig. 3, Fig.6(a) and Fig. 7(a) was listed and compared with each other. Clearly, these three models have a similar linear relationship.

Then, from Fig. 8(b), we demonstrated that model# 2 was also almost the same in the three different solutions.

Although the model# 3 has the different formula when using different solutions (Fig. 8(c)), as what we did above, a new model # 3 can be built based on the composition and

TABLE 2. Parameters of droplets used for electrolysis reactions.

Model #	Min. (D_e)	Max. (D_e)	Increments	Droplet number
1	962.5 μm	1665.3 μm	0.4 μL	5
2	1502.6 μm	1502.6 μm	0	7
3	1502.6 μm	1502.6 μm	0	6

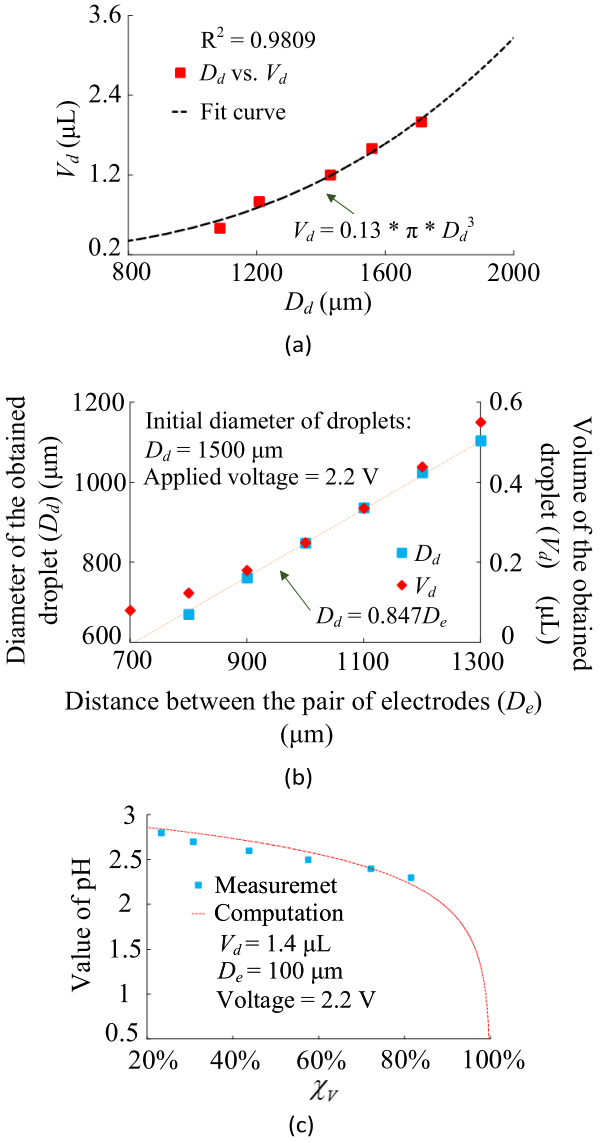

FIGURE 7. Demonstration of model# 1, 2 and 3 in the H_2SO_4 solution (0.001mol/L). (a) Relationship between the droplet's volume and its diameter. (b) Electrodes' distance vs. droplets' diameter. (c) The relationship between the resulted pH value and X_V.

mass ratio of the solution before and after the electrolysis reaction even if other solutions are used. Here, the H_2SO_4 solution used in the experiments has an initial concentration of 0.001 mol/L. With this value, the pH value is about 3. We did not further continue to electrolyze the droplets when

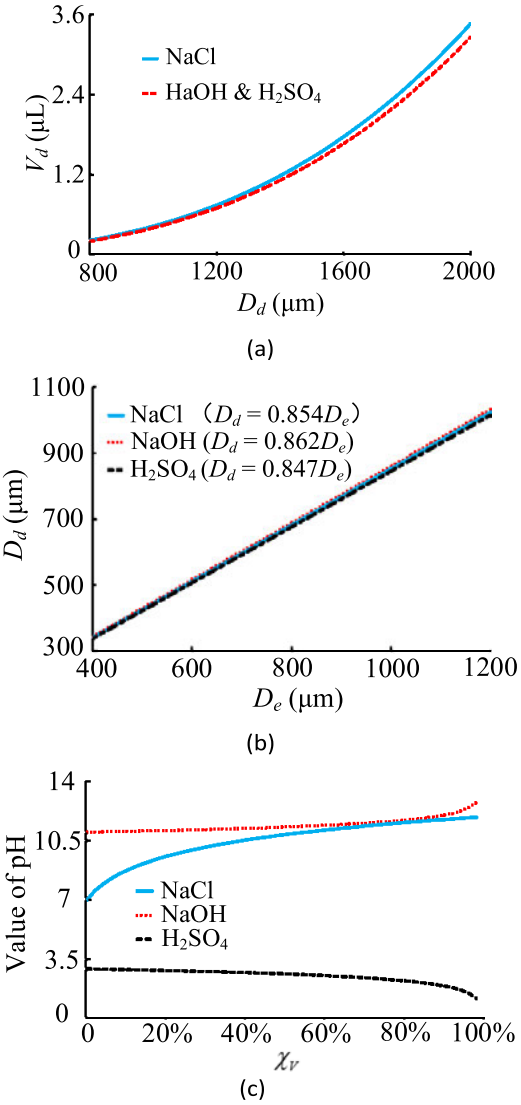

FIGURE 8. Comparison of model# 1, 2 and 3 in the sodium chloride solution (5%), NaOH solution (0.001 mol/L) and H_2 SO_4 solution (0.001 mol/L). (a) The droplet's volume vs. its diameter. (b) Electrodes' distance vs. droplets' diameter. (c) The relationship between the resulted pH value and X_V.

the pH value is close to 1.2. With the pH value, the left volume is only 1.1% of the initial value. If we want to get a droplet with the pH value close to 0, the better way is to make a new H_2SO_4 solution with a higher concentration and then to electrolyze it. To NaOH solution, if we want to form a droplet with the pH value close to 14, the above method also can be used. However, to the NaCl solution, the above method loses effect. To form a droplet with the pH value higher than 12.2, we need to continue to electrolyze it which means to consume more solutions and take much more time. Thus, to the different solutions, forming a solution with desired pH values in the model#3, we need to select an effective method and simultaneously make a balance among the χ_v, reaction time and the initial and the resulted pH values. The operations above need to be conducted to the solutions with good electrical conductivity.

IV. CONCLUSION

This paper proposed a low-cost, high-efficient strategy capable of modifying the size of droplets and synchronously adjusting their pH values as demand based on the electrolysis reactions in silicone oil, which is unable or very difficult to be achievable before our study. Three models, the relationship between the droplet's volume and its diameter, the relationship between the distance of two electrodes and the size of the resulted micro-droplet, and the relationship between the pH value of the micro-droplets consuming rate, were built. Our experiments demonstrated that the models ensured that the electrolysis relations can stop automatically when the resulted droplet has reached the desired volume and pH value.

In the future, we intend to promote the proposed method to many different types of conductive solutions, increasing its application fields, such as analytical chemistry, precision engineering, etc.

REFERENCES

[1] W. H. Chong, Y. Huang, T. N. Wong, K. T. Ooi, and G.-P. Zhu, "Magnetic nanorobots, generating vortexes inside nanoliter droplets for effective mixing," *Adv. Mater. Technol.*, vol. 3, no. 4, Apr. 2018, Art. no. 1700312.

[2] Z. Wang, H. Zhang, Y. Yang, H. Qu, Z. Han, W. Pang, and X. Duan, "Wireless controlled local heating and mixing multiple droplets using micro-fabricated resonator array for micro-reactor applications," *IEEE Access*, vol. 5, pp. 25987–25992, Oct. 2017.

[3] G. Wang, J. Deng, and X. Guo, "Electrohydrodynamic assisted droplet alignment for lens fabrication by droplet evaporation," *J. Appl. Phys.*, vol. 123, no. 16, Apr. 2018, Art. no. 163102.

[4] A. Z. Giovannini, N. Gambino, B. Rollinger, and R. S. Abhari, "Angular ion species distribution in droplet-based laser-produced plasmas," *J. Appl. Phys.*, vol. 117, no. 3, Jan. 2015, Art. no. 33302.

[5] S. A. Reijers, D. Kurilovich, F. Torretti, H. Gelderblom, and O. O. Versolato, "Laser-to-droplet alignment sensitivity relevant for laser-produced plasma sources of extreme ultraviolet light," *J. Appl. Phys.*, vol. 124, no. 1, Jul. 2018, Art. no. 13102.

[6] M. Duocastella, C. Florian, P. Serra, and A. Diaspro, "Sub-wavelength laser nanopatterning using droplet lenses," *Sci. Rep.*, vol. 5, Nov. 2015, Art. no. 16199.

[7] O. Kurochkin, "Ultra-fast adaptive optical micro-lens arrays based on stressed liquid crystals," *J. Appl. Phys.*, vol. 124, Dec. 2018, Art. no. 214501.

[8] J. Zhang, "Fundamentals and applications of inertial microfluidics: A review," *Lab Chip*, vol. 16, pp. 10–34, Nov. 2016.

[9] A. S. Hansen, N. Hao, and E. K. O'Shea, "High-throughput microfluidics to control and measure signaling dynamics in single yeast cells," *Nature Protocols*, vol. 10, no. 8, pp. 1181–1197, 2015.

[10] P. Pouponneau, J.-C. Leroux, and S. Martel, "Magnetic nanoparticles encapsulated into biodegradable microparticles steered with an upgraded magnetic resonance imaging system for tumor chemoembolization," *Biomaterials*, vol. 30, pp. 6327–6332, Oct. 2009.

[11] F. Beroz, L. M. Jawerth, S. Münster, D. A. Weitz, C. P. Broedersz, and N. S. Wingreen, "Physical limits to biomechanical sensing in disordered fibre networks," *Nature Commun.*, vol. 8, Jul. 2017, Art. no. 16096.

[12] A. Asada, H. Aoki, H. Kurita, A. Antoniu, H. Yasuda, K. Takashima, and A. Mizuno, "A novel gene transformation technique using water-in-oil droplet in an electrostatic field," *IEEE Trans. Ind. Appl.*, vol. 49, no. 1, pp. 311–315, Jan./Feb. 2013.

[13] H. Zhao, X. Guo, Y. Wang, X. Duan, H. Qu, H. Zhang, D. Zhang, and W. Pang, "Microchip based electrochemical-piezoelectric integrated multi-mode sensing system for continuous glucose monitoring," *Sens. Actuators B, Chem.*, vol. 223, pp. 83–88, Feb. 2016.

[14] L. Zhang, H. Liu, Y. Zhao, X. Sun, Y. Wen, Y. Guo, X. Gao, C.-A. Di, G. Yu, and Y. Liu, "Inkjet printing high-resolution, large-area graphene patterns by coffee-ring lithography," *Adv. Mater.*, vol. 24, pp. 436–440, Jan. 2012.

[15] M. Singh, H. M. Haverinen, P. Dhagat, and G. E. Jabbour, "Inkjet printing-process and its applications," *Adv. Mater.*, vol. 22, no. 6, pp. 673–685, 2010.

[16] C. Keum, "Principle of topography-directed inkjet printing for functional micro-tracks in flexible substrates," *J. Appl. Phys.*, vol. 121, Jun. 2017, Art. no. 244902.

[17] A. S. Gladman, "Biomimetic 4D printing," *Nature Mater.*, vol. 15, pp. 413–419, Jan. 2016.

[18] R. C. Rodrigues, C. Ortiz, Á. Berenguer-Murcia, R. Torres, and R. Fernández-Lafuente, "Modifying enzyme activity and selectivity by immobilization," *Chem. Soc. Rev.*, vol. 42, pp. 6290–6307, Oct. 2012.

[19] G. Isaksson, I. Lundquist, and I. Ihse, "Effect of dietary fiber on pancreatic enzyme activity in vitro: The importance of viscosity, pH, ionic strength, adsorption, and time of incubation," *Gastroenterology*, vol. 82, no. 5, pp. 918–924, 1982.

[20] S. Sood, R. Peelamedu, K. B. Sundaram, E. Dein, and R. M. Todi, "Wet etching of sputtered tantalum thin films in NaOH and KOH based solutions," *J. Mater. Sci., Mater. Electron.*, vol. 18, pp. 535–539, May 2007.

[21] T. L. Andresen, S. S. Jensen, and K. Jørgensen, "Advanced strategies in liposomal cancer therapy: Problems and prospects of active and tumor specific drug release," *Progr. Lipid Res.*, vol. 44, no. 1, pp. 68–97, Jan. 2005.

[22] L. Jiang, L. Li, X. He, Q. Yi, B. He, J. Cao, W. Pan, and Z. Gu, "Overcoming drug-resistant lung cancer by paclitaxel loaded dual-functional liposomes with mitochondria targeting and pH-response," *Biomaterials*, vol. 52, pp. 126–139, Jun. 2015.

[23] F. Danhier, O. Feron, and V. Préat, "To exploit the tumor microenvironment: Passive and active tumor targeting of nanocarriers for anti-cancer drug delivery," *J. Controlled Release*, vol. 148, no. 2, pp. 135–146, Dec. 2010.

[24] A. Vashist, A. Vashist, Y. K. Gupta, and S. Ahmad, "Recent advances in hydrogel based drug delivery systems for the human body," *J. Mater. Chem. B*, vol. 2, no. 2, pp. 147–166, 2014.

[25] M. Z. Miskin, K. J. Dorsey, B. Bircan, Y. Han, D. A. Muller, P. L. McEuen, and I. Cohen, "Graphene-based bimorphs for micron-sized, autonomous origami machines," *Proc. Nat. Acad. Sci. USA*, vol. 115, no. 3, pp. 466–470, Jun. 2018.

[26] L. Zhou, A. E. Marras, C.-M. Huang, C. E. Castro, and H.-J. Su, "Paper origami-inspired design and actuation of DNA nanomachines with complex motions," *Small*, vol. 14, Nov. 2018, Art. no. 1802580.

[27] T. A. Kowalewski, "On the separation of droplets from a liquid jet," *Fluid Dyn. Res.*, vol. 17, pp. 121–145, Feb. 1996.

[28] D. R. Link, S. L. Anna, D. A. Weitz, and H. A. Stone, "Geometrically mediated breakup of drops in microfluidic devices," *Phys. Rev. Lett.*, vol. 92, no. 5, Feb. 2004, Art. no. 054503.

[29] J.-C. Baret and F. Mugele, "Electrical discharge in capillary breakup: Controlling the charge of a droplet," *Phys. Rev. Lett.*, vol. 96, no. 1, Jan. 2006, Art. no. 016106.

[30] R. T. Collins, J. J. Jones, M. T. Harris, and O. A. Basaran, "Electrohydrodynamic tip streaming and emission of charged drops from liquid cones," *Nature Phys.*, vol. 4, pp. 149–154, Dec. 2008.

[31] P. B. Umbanhowar, V. Prasad, and D. A. Weitz, "Monodisperse emulsion generation via drop break off in a coflowing stream," *Langmuir*, vol. 16, pp. 347–351, Oct. 2000.

[32] K. Li, J. Liu, W. Chen, and L. Zhang, "Influences of excitation on droplet spreading characteristics ejected by piezoelectric micro-jet," *IEEE Access*, vol. 6, pp. 25930–25938, Mar. 2018.

[33] L. Yobas, S. Martens, W.-L. Ong, and N. Ranganathan, "High-performance flow-focusing geometry for spontaneous generation of monodispersed droplets," *Lab Chip*, vol. 6, pp. 1073–1079, May 2006.

[34] E. Castro-Hernández, P. García-Sánchez, S. H. Tan, A. M. Gañáán-Calvo, J.-C. Baret, and A. Ramos, "Breakup length of AC electrified jets in a microfluidic flow-focusing junction," *Microfluidics Nanofluidics*, vol. 19, pp. 787–794, Jun. 2015.

[35] F. Malloggi, S. A. Vanapalli, H. Gu, D. van den Ende, and F. Mugele, "Electrowetting-controlled droplet generation in a microfluidic flow-focusing device," *J. Phys., Condens. Matter*, vol. 19, no. 46, 2007, Art. no. 462101.

[36] A. Ray, "On demand manipulation of ferrofluid droplets by magnetic fields," *Sens. Actuators B, Chem.*, vol. 242, pp. 760–768, Apr. 2016.

[37] P. Irajizad, N. Farokhnia, and H. Ghasemi, "Dispensing nano-pico droplets of ferrofluids," *Appl. Phys. Lett.*, vol. 107, Nov. 2015, Art. no. 191601.

[38] S. M. S. Murshed, S. H. Tan, N. T. Nguyen, T. N. Wong, and L. Yobas, "Microdroplet formation of water and nanofluids in heat-induced microfluidic T-junction," *Microfluidics Nanofluidics*, vol. 6, no. 2, pp. 253–259, Feb. 2009.

[39] Y. F. Yap, "Thermally mediated control of liquid microdroplets at a bifurcation," *J. Phys. D, Appl. Phys.*, vol. 42, Mar. 2009, Art. no. 065503.

[40] L. Schmid and T. Franke, "SAW-controlled drop size for flow focusing," *Lab Chip*, vol. 13, no. 9, pp. 1691–1694, Feb. 2013.
[41] T. Franke, A. R. Abate, D. A. Weitz, and A. Wixforth, "Surface acoustic wave (SAW) directed droplet flow in microfluidics for PDMS devices," *Lab Chip*, vol. 9, no. 18, pp. 2625–2627, Jun. 2009.
[42] C.-T. Chen and G.-B. Lee, "Formation of microdroplets in liquids utilizing active pneumatic choppers on a microfluidic chip," *J. Microelectromech. Syst.*, vol. 15, no. 6, pp. 1492–1498, Dec. 2006.
[43] H. Willaime, V. Barbier, L. Kloul, S. Maine, and P. Tabeling, "Arnold tongues in a microfluidic drop emitter," *Phys. Rev. Lett.*, vol. 96, Feb. 2006, Art. no. 054501.
[44] W. Wen, X. Huang, S. Yang, K. Lu, and P. Sheng, "The giant electrorheological effect in suspensions of nanoparticles," *Nature Mater.*, vol. 2, pp. 727–730, Oct. 2003.
[45] Z. Chong, S. H. Tan, A. M. Gañán-Calvo, S. B. Tor, N. H. Loh, and N.-T. Nguyen, "Active droplet generation in microfluidics," *Lab Chip*, vol. 16, pp. 35–58, Oct. 2015.
[46] S. Y. Park, T.-H. Wu, Y. Chen, M. A. Teitell, and P.-Y. Chiou, "High-speed droplet generation on demand driven by pulse laser-induced cavitation," *Lab Chip*, vol. 11, no. 6, pp. 1010–1012, 2011.

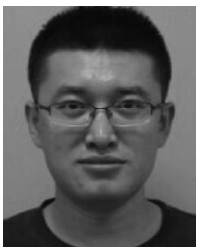

GENGCHAO CHEN received the B.C. degree in applied physics and the M.E. degree in mechanics engineering from the Nanjing University of Aeronautics and Astronautics (NUAA), Nanjing, China, in 2011 and 2014, respectively. He is currently pursuing the Ph.D. degree with the South China University of Technology (SCUT), Guangzhou, China.

XIANMIN ZHANG received the Ph.D. degree in mechanical engineering from the Beijing University of Aeronautics and Astronautics, Beijing, China, in 1993.

He has been the Director of the Guangdong Provincial Key Laboratory of Precision Equipment and Manufacturing Technology, since 2010, and has also been the Dean and the Chair Professor with the School of Mechanical and Automotive Engineering, South China University of Technology, since 2013. His research interests include robotics, precision instrument analysis and design, and dynamics and vibration control of mechanisms. He has finished more than 50 projects and authored or coauthored more than 300 technical papers. He holds more than 100 patents.

Dr. Zhang has been serving as the Chair for the China Committee of the International Federation for the Promotion of Mechanism and Machine Science, since 2016.

NING LI was born in Xintai, Taian, Shandong, China, in 1987. He received the B.S. degree in mechanical engineering from Naval Aeronautical Engineering Academy, Qingdao, China, in 2009, the M.S. degree in mechanical engineering from the Nanjing University of Aeronautics and Astronautics, Nanjing, China, in 2012, and the Ph.D. degree from the École Polytechnique de Montréal, Université de Montréal, Montréal, Canada, in 2019.

He is currently a Postdoctoral Fellow with the Le Centre de recherche du CHUM (CRCHUM), Université de Montréal.